

Effects of Annealing Temperature on Infrared Spectra of SiO₂ Extracted From Rice Husk

M. H. Shahrokh Abadi*¹, A. Delbari¹, Z. Fakoor¹, J. Baedi²

¹Electronic Dept. of Electrical and Computer Engineering
Faculty, Hakim Sabzevari University, Sabzevar, Iran

²Physics Dept. of Science Faculty, Hakim Sabzevari University, Sabzevar, Iran

received July 17, 2014; received in revised form August 29, 2014; accepted September 27, 2014

Abstract

The effects of the annealing temperature on the structures and quantities of silicon dioxide obtained from rice husk by means of thermal treatment followed by acid leaching were studied with infrared transmission in the wavenumber range 400–4000 cm⁻¹. The Fourier Transform Infrared Radiometer (FTIR) spectra of five series of samples including rice husk, rice husk ash burnt at 800 °C, and rice husk ash annealed at 900, 1000, and 1100 °C were analyzed and compared. It was demonstrated that the main absorption Si-O-Si bending band shifts towards lower wavenumbers while the peaks of stretching and rocking bands of Si-O-Si monotonically shift toward higher wavenumbers as the annealing temperature is increased. Analysis of the transmission samples showed that the shape of Si-O-Si bonds changes owing to the annealing temperature, varying in the range of 8 to 40 cm⁻¹.

Keywords: FTIR, transmittance, SiO₂, rice husk, bond structure, stretching, bending, rocking.

I. Introduction

Silicon dioxide (SiO₂), a key material in the electronics industry, is the repeating general structure formula of most rocks, occurring commonly in nature as sandstone, silica sand or quartzite. SiO₂ is crystallized in three main forms – quartz, tridymite, and cristobalite. The structure of quartz is a three-dimensional network of 6-membered Si-O rings, like three SiO₄ tetrahedra^{1, 2}.

SiO₂ also can be found in some agro-products such as rice husk (RH). It contains 13–29% inorganic components, of which 87–97% is SiO₂ in an amorphous state³. The extraction of SiO₂ from residual rice husk has interested many researchers working on the basis two main applications: 1) Semi-conductor-related material based on purification of extracted SiO₂ and Si conversion, 2) Cement industry and mainly lightweight construction products^{4, 5}. Highly purified product is needed in the former application and the process is usually conducted by burning the RH above 500 °C to white ash followed by acid leaching to obtain rice husk ash (RHA). The presence of amorphous and crystalline SiO₂ in the RHA depends on the thermal treatment in the process, in which the structure can be transformed into crystalline form in the temperature range 900–1300 °C, and varies from quartz to tridymite to cristobalite^{6–9}.

Structure of a compound is normally estimated and quantified using Fourier Transform Infrared Spectroscopy (FTIR) by investigating absorbed IR through the molecules of a sample, which in turn is translated to the interatomic vibrational energy of the atoms compris-

ing the molecules, either in the form of stretching or bending^{10–12}. The absorption or transmission results from coupling of a dipole vibration with the electric field of the infrared radiation. The absorption due to a particular dipole oscillation is generally not greatly affected by other atoms present in the molecule. Thus the absorption occurs at approximately the same frequency for all bonds in different molecules^{13–15}.

In this study, the presence and characteristics of SiO₂ in RH, RHA burnt at 800 °C, and a series of RHA annealed at temperatures of 900, 1000, and 1100 °C were examined structurally and quantitatively by analyzing the SiO₂ content based on the transmittance method of FTIR.

II. Materials and Methods

The raw material used for this study was rice husk (RH) purchased from a local farm (Babol, Mazandaran Province, Northern Iran). The first step to produce the SiO₂ from RH consisted of washing the RH with tap water and drying it in the sunlight to vaporize the water content. The next step involved acid-leaching with diluted hydrochloric acid (HCl) in distilled water (2 : 8) and then drying the RH at room temperature (RT). The aim of these initial steps was to remove any soil and dirt from the RH. The dried RH was then burnt inside a beaker using a resistive furnace to obtain a brown rice husk ash (RHA). The RHA was ground in an agate mortar to reduce the mean particle size. Then by means of thermal treatment in a tube furnace with atmospheric conditions (from room temperature to 800 °C, rate 5 /min, held at the maximum temperature for 3 h), the brown RHA was transformed

* Corresponding author: mhshahrokh@hsu.ac.ir

into white RHA. This was done to increase the specific surface area (SSA) of the SiO_2 and remove any unwanted chemical compounds from the ash. To minimize the effects of phase transitions and crystal defects owing to the exothermicity of SiO_2 , the heating process of the ash was also defined at 10 min at 200 °C and 400 °C and 60 min at 600 °C. Then the ash was divided into four samples. Using same profile as for the heating process, an annealing profile was applied to three samples at the maximum temperatures of 900, 1000, and 1100 °C, respectively. The last sample remained untreated. Eventually, the four samples including an RH sample were used for FTIR analysis. Fig. 1 shows a thermal treatment profile as an example.

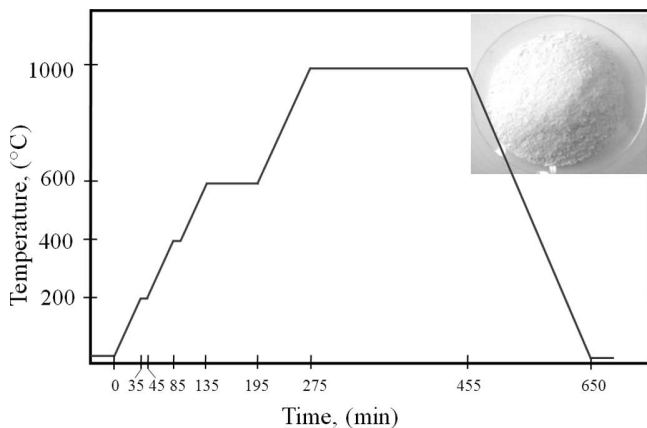


Fig. 1: A sample thermal treatment profile. Inset shows produced white RHA.

III. Results and Discussion

Fourier Transform Infrared Spectroscopy was performed using a Shimadzu 8400S FTIR spectrometer in transmission (T) mode at mid IR, wavenumbers range 400–4000 cm^{-1} ($\lambda = 2.5 - 25 \mu\text{m}$), to conduct IR measurements. Band intensities can be also expressed in absorbance mode, in which same results are expected. Absorption of radiant energy is represented by a “trough” in the curve which means zero transmittance corresponds to 100 % absorption of light at that wavelength. Absorbance is the logarithm, to the base 10, of the reciprocal of the transmittance, i.e. $A = \log_{10}(1/T)$.

For the analysis, samples were ground to a fine powder consisting of particles of 2 μm or less, lower than the end of radiation wavelength, to minimize band distortion owing to scattering of radiation. The powder was then dispersed in a matrix of potassium bromide (KBr) in the ratio of ~1 : 100 and finally transferred to a die with an average thickness of 0.12 mm. KBr absorbs moisture from the atmosphere and does have some fundamental transitions at ~1660 cm^{-1} . The absorption coefficient of KBr is far less than 400 cm^{-1} , therefore no absorption peak of KBr appeared in the range of measurement.

In the IR spectra of SiO_2 ; rocking, bending, and stretching vibrational bands of Si-O can be observed at ~450 cm^{-1} , ~800 cm^{-1} , and ~1080 cm^{-1} , respectively¹⁶. Since the thickness of the samples is already known, the concentration of interstitial oxygen in silicon at these bands can be calculated based on the Fabry-Perot method with Eq. (1):

$$O_i = \frac{O_{i,\text{Absorp.Coeff}} \times \text{Absorbance}}{\text{SampleThickness(cm)}} \times \ln 10 (\text{atoms/cm}^3) \quad (1)$$

Fig. 2 (a) shows the transmittance intensities of the samples with detail of the intensity of transmittance peaks at wavenumbers ranging between 400 and 4000 cm^{-1} . An IR transmittance correlation chart of SiO_2 is also given in Fig. 2 (b) as the reference. The appearance of strong absorption bands in the region of 4000 to 1400 cm^{-1} usually comes from stretching vibrations between hydrogen and some other atoms and a wide variety of double- and triple-bonded functional groups such as carbonyls and alkenes. The IR spectra produced with the pellet technique often exhibit bands at 3450 cm^{-1} and 1640 cm^{-1} owing to absorbed moisture.

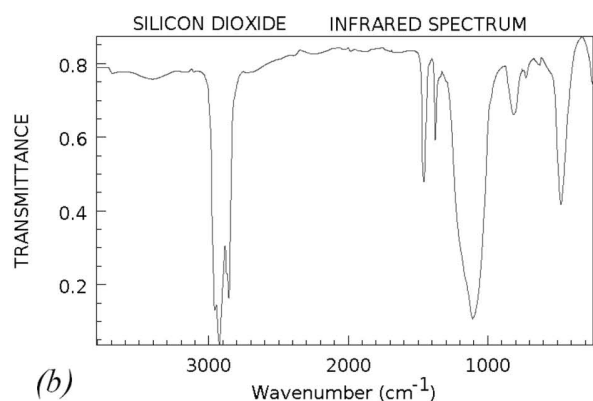
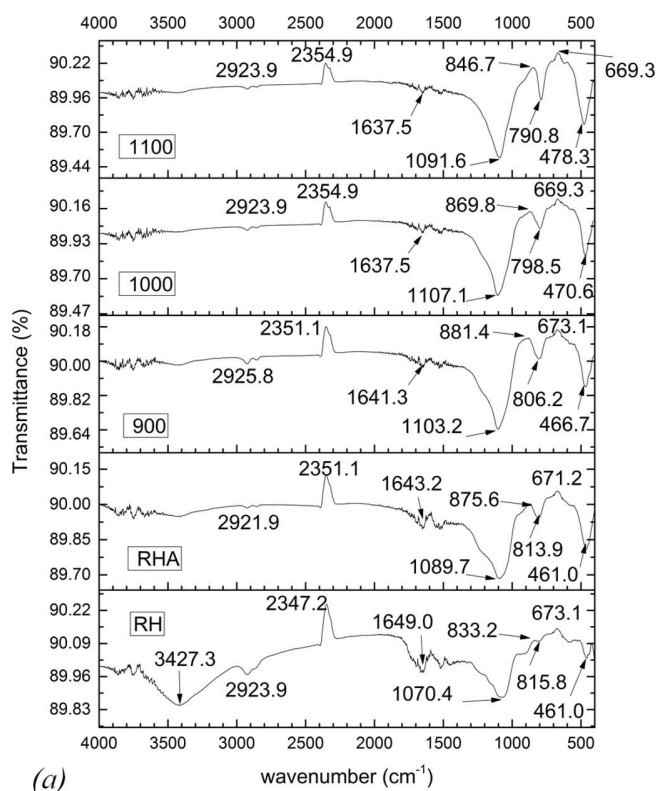


Fig. 2: (a) Transmittance representative FTIR spectra of different samples; RH, RHA, 900 °C, 1000 °C, and 1100 °C from bottom to the top, respectively. Numbers indicate the wave numbers of peaks of interest in cm^{-1} , (b) IR correlation chart of SiO_2 adapted from National Institute of Standards and Technology (NIST) source reference COBLENTZ No. 5585.

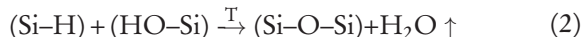
Referring to Fig.2 (a), a broad band of vibrational stretching owing to the O-H bond is observed at ~3427 cm⁻¹ significantly in RH and RHA. The existence of the bond is pervasive owing to the adsorption properties on the surface of silica and related silicates, referred to as silanol bond, a single compound with the formula H₃SiOH¹⁷. The strength of the bond dramatically decreased owing to dehydroxylation as the treatment temperature of the samples was increased, resulting in the change in the relative band intensities and shift to lower wavenumbers. The shift is correlated to the concentration of H-bonded silanols relative to that of isolated silanols¹⁸. Owing to the water absorption at higher temperatures, the highly porous structure may accommodate the volume change, becoming a denser structure.

Another vibrational stretching assigned to hydroxyl functional group of C-O-H, related to trimethylsilanol, can be observed at ~2923 cm⁻¹. It reacts with the silanol groups of the higher wavenumbers and coats the surface of the sample with a layer of hydrophobic methyl groups¹⁹. The content of carbon in the bond is responsible for varying band intensities, which is not of interest in this analysis. A C-H vibrational stretching band, owing to the absence of SiH, is also observed at ~2355–2347 cm⁻¹ and assigned to either symmetrical or asymmetrical CH₂ bonds. This indicates a carbon-rich termination for the cubic hydrogen-annealed surfaces, as it has been suggested by Seyller²⁰ that the higher annealing temperature, the higher intensity of the bond to the lower wavenumbers.

Fig. 3 shows the next range of interest with more details expanded from 1650 to 1590 cm⁻¹. In this region, vibrational bending H-OH bond of adsorbed water molecules can be seen at ~1649–1637 cm⁻¹. As suggested by Adam and Chua²¹ the water molecules are unable to escape from the silica matrix, therefore small peaks of the bonds were present in the samples annealed at higher temperatures and the peaks are shifted to lower wavenumbers accordingly. The next peak of interest occurs at ~1600–1591 cm⁻¹ and is ascribed to C-O vibrational bending. Furthermore, it can be seen from Fig. 3 that there are no significant changes between the peak intensities and their associated wavenumbers of samples annealed at 1000 and 1100 °C in the given range.

Both IR spectra of transmittance and absorbance vibrational bonds of Si are shown in Fig. 4 in the wavenumbers range 400–1400 cm⁻¹. The IR spectra of Si-O-Si are often presented in this range to characterize vibrational absorption modes of the Si-O-Si unit and furthermore, to investigate the phase separation and silicon crystallization of the silica-based samples²². Therefore, instead of transmittance mode, the absorption mode of the FTIR results is taken into account. Fig. 4 (b) shows the vibrational absorption stretching, bending, and rocking bonds of Si-O-Si. The series bands at ~1110–1070 cm⁻¹ are interpreted ow-

ing to the Si-O-Si asymmetric stretching vibration bond. The band shifts slightly to higher wavenumbers as the annealing temperature is increased. The shift is reversed for the sample annealed at 1100 °C. It is presumed that this happens because of the tighter bonds owing to the densification of SiO₂ and it is predicted that at higher temperature the band would shift to a wavenumber as low as 1090 cm⁻¹. The increase in the amount of Si-O-Si could result from condensation reaction of the silanol groups and is called as organosilicate. The reaction is thermally activated and needs enough Si-OH bonds to make the group of Si-O-Si²³:



As the temperature is increased the water content is vaporized and the structure is presumed to be porous.

The bands at ~815–790 cm⁻¹ are assigned to a network vibrational bending Si-O-Si symmetric bonds^{23, 24}. The band shifts slightly to lower wavenumbers as the annealing temperature is increased. The bands at ~478–460 cm⁻¹ are associated with a network of Si-O-Si bond rocking modes²⁴. In the case of crystalline SiO₂, formation of a new bond at ~669 cm⁻¹ is due to the polymerization of the cristobalite phase of silicates, and is described as structure-dependent Si-O-Si symmetrical bending vibrations²⁵.

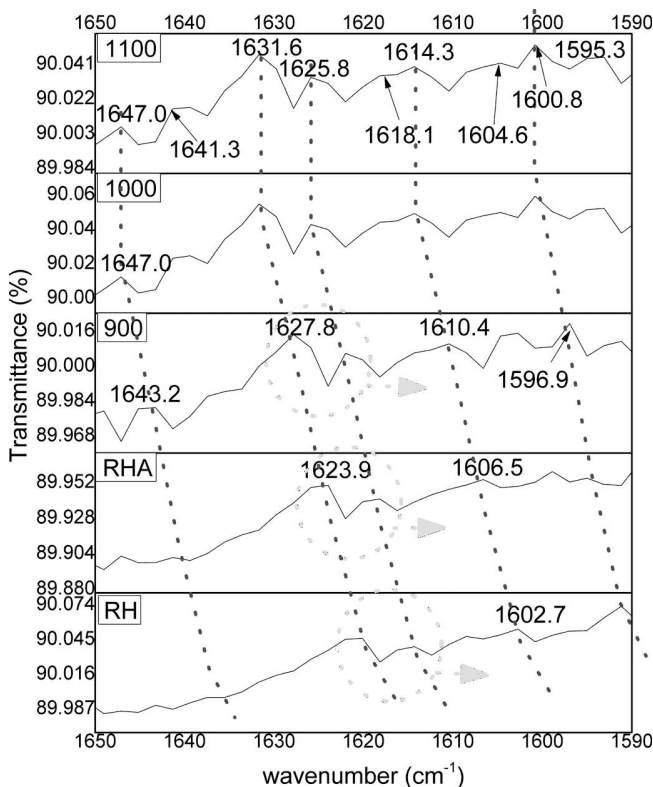


Fig. 3: An expanded detail of transmittance spectra of the samples range 1650 to 1590 cm⁻¹, indicates the H-OH and C-O bonds. Adsorption peaks tend to shift to lower wave numbers when the annealing temperature is lower than 900 °C.

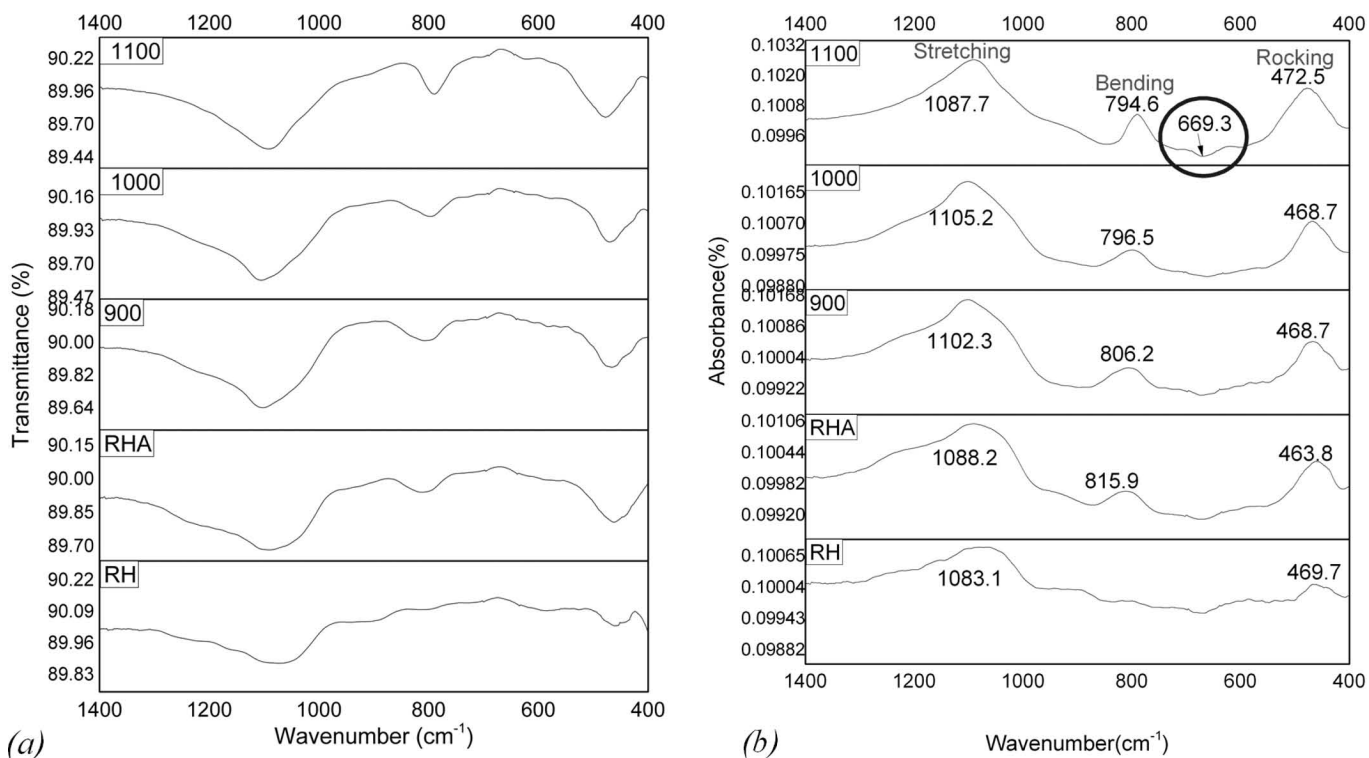


Fig. 4: IR (a) transmittance vs. (b) absorbance spectra of vibrational Si bonds.

IV. Conclusions

We examined the effect of the annealing temperature on the infrared spectra of rice husk, rice husk ash, and rice husk ash annealed at 900, 1000, and 1100 °C. We showed that the silanol and the hydro-carbonaceous contents decrease with increasing annealing temperature owing to a dehydroxylation process as suggested in Eq. (2). We also showed that the intensity of the absorption bands as well as their associated wavenumbers were altered with the annealing temperature. As evidence, these alterations can be seen at the bands located at $\sim 1070\text{--}1110\text{ cm}^{-1}$, $\sim 815\text{--}790\text{ cm}^{-1}$, and $\sim 460\text{--}478\text{ cm}^{-1}$. The effect of the annealing process was more pronounced for the absorption case of 1100 °C at $\sim 1110\text{ cm}^{-1}$. It is concluded that rice husk as an agriculture product residue is a good substitution to produce high-quality SiO_2 provided care is taken during the annealing process.

Acknowledgements

The authors are thankful to Ms Z. Banihashemi for her great cooperation in the Chemophysics Lab, taking IR measurements, and also to Mr Qanei for his support in the Solid-State Lab, Faculty of Science, Hakim Sabzevari University.

References

- 1 Carraher, C.E.: Giant molecules: essential materials for everyday living and problem solving, 2nd edition, John Wiley & Sons, Inc., New York, 2003.
- 2 Douglas, B., Ho, S.-M.: Structure and chemistry of crystalline solids: crystal structures of silica and metal silicates, Springer, New York, 2006.
- 3 Zakharov, A.I., Belyakov, A.V., Trviginov, A.N.: Forms of extraction of silicon compounds in rice husks, *Glass Ceram.*, **50**, 420–425, (1993).
- 4 Gorthy, P., Mukunda Pudukottah, G.: Production of silicon carbide from rice husks, *J. Am. Ceram. Soc.*, **82**, 1393–1400, (1999).
- 5 Real, C., Alcala, M.C., Cariado, J.M.: Preparation of silica from rice husks, *J. Am. Ceram. Soc.*, **79**, 2012–2016, (1996).
- 6 Kordatos, K., Gavela, S., Ntziouni, A., Pistiolas, K.N., Kyritsi, A., Kasselouri, V.: Synthesis of highly siliceous ZSM-5 zeolite using silica from rice husk ash, *Micropor. Mesopor. Mat.*, **115**, 189–196, (2008).
- 7 Shinohara, Y., Kohyama, N.: Quantitative analysis of tridymite and cristobalite crystallized in rice husk ash by heating, *Ind. Health*, **42**, 277–285, (2004).
- 8 Amick, J.A.: Purification of rice hulls as a source of solar grade silicon for solar cells, *J. Electrochem. Soc.*, **129**, 864–866, (1982).
- 9 Zhuravlev, L.T.: The surface chemistry of amorphous silica. zhuravlev model, *Colloid. Surface*, **173**, 1–38, (2000).
- 10 Tomita, K., Kawano, M.: Effect of cations on crystallization of amorphous silica (part 1), *Earth Sci. & Biology*, **25**, 1–18, (1992).
- 11 Kumar, A., Mohanta, K., Kumar, D., Parkash, O.: Properties and industrial applications of rice Husk: A review, *Int. J. of Emerging Tech. and Advanced Engineering*, **2**, 86–90, (2012).
- 12 Venezia, A.M., Parola, V., Longo, A., Martorana, A.: Effect of alkali ions on the amorphous to crystalline phase transition of silica, *J. Solid State Chem.*, **161**, 373–378, (2001).
- 13 Javed, S.H., Naveed, S., Feroze, N., Zafar, M., Shafaq, M.: Crystal and amorphous silica from KMnO_4 Treated and untreated rice husk, *J. of Quality and Tech. Management*, **6**, 81–90, (2010).
- 14 Dongmin, A., Yupeng, G., Bo, Z., Yanchao, Z., Zichen, W.: A study on the consecutive preparation of silica powders and active carbon from rice husk ash, *Biomass Bioenerg.*, **5**, 1227–1234, (2011).
- 15 Samah, B.D., Hilmi, M., Maizatul, S.S.: Effect of organic and inorganic acid pretreatment on structural properties of rice husk and adsorption mechanism of phenol. *Int. J. of Chem. and Env. Eng.*, **3**, 192–200, (2012).

- 16 Moore, C., Perova, T.S., Kennedy, B.J., Berwick, K., Shaganov, I.I., Moore, R.A.: Study of structure and quality of different silicon oxides using FTIR and Raman microscopy. *In OPTO Ireland International Society for Optics and Photonics*, 1247–1256, (2003).
- 17 Chandrasekhar, V., Boomishankar, R., Nagendran, S.: Recent developments in the synthesis and structure of organosilanol, *Chem. Rev.*, **104**, 5847–5910, (2004).
- 18 Gillis-D'Hamers, I., Vrancken, K.C., Vansant, E.F., De Roy, G.: Fourier-transform infrared photo-acoustic spectroscopy study of the free hydroxyl group vibration, *J. Chem. Soc., Faraday Trans*, **88**, 2047–2050, (1992).
- 19 Grubb, W.T., Osthoff, R.C.: Physical properties of organosilicon Compounds. II. trimethylsilanol and triethylsilanol, *J. Am. Chem. Soc.*, **75**, 2230–2232, (1953).
- 20 Thomas Seyller: Passivation of hexagonal SiC surfaces by hydrogen termination, *J. Phys.: Condens. Matter*, **16**, 1755–1761, (2004).
- 21 Adam, F., Chua, J.-H.: The adsorption of palmytic acid on rice husk ash chemically modified with Al(III) ion using the sol-gel technique, *J. Colloid Interf. Sci.*, **280**, 55–61, (2004).
- 22 Nobuyoshi Koshida: Device applications of silicon nanocrystals and nanostructures. Springer Science & Business Media, New York, 2009.
- 23 Baklanov, M., Ho, P.S., Zschech, E.: Advanced interconnects for ULSI technology, John Wiley & Sons, New York, 2011.
- 24 Bange, J.P., Patil, L.S., Gautam, D.K.: Growth and characterization of SiO₂ films deposited by flame hydrolysis deposition system for photonic device application, *Prog. Electromag. Res. M.*, **3**, 165–175, (2008).
- 25 Mazo, M.A., Tamayo, A., Rubio, F., Soriano, D., Rubio, J.: Effect of processing on the structural characteristics of sintered silicon oxycarbide materials, *J. Non-Cryst. Solids*, **391**, 23–31, (2014).

